Electronic Supplementary Material (ESI) for Dalton Transactions.
This journal is © The Royal Society of Chemistry 20xx

Supporting Information

Cluster nuclearity control and modulated hydrothermal synthesis of functionalized Zr_{12} metal-organic frameworks

Shing Bo Peh,[a] Youdong Cheng,[a] Jian Zhang,[a] Yuxiang Wang,[a] Ger Hui Chan,[a] Jian Wang,[a] and Dan Zhao*,[a]

[a] Department of Chemical and Biomolecular Engineering, National University of Singapore, 4 Engineering Drive 4, 117585 Singapore

Table of Contents

Experimental

Materials

All the chemicals were obtained from commercial sources and used without further purification. The ultrapure water was supplied by a water purification system, PU$^+$.

Synthesis of Zr-MOFs with Zr_{12} clusters. Briefly, $ZrOCl_2 \cdot 8H_2O$ (metal salt) was dissolved in solvent to yield a homogeneous metal salt solution. The solid ligand was introduced into Teflon liners. Subsequently, the salt solution was introduced, followed by variable amounts of acetic acid (AA) as the modulator (Note: for most cases, formic acid may be employed as an alternative with similar phase behavior). The reaction mixture was briefly homogenized by sonication. Sealed autoclaves were kept in a preheated isothermal oven at the specified temperature. The solid products were recovered by centrifugation and washed copiously with deionized (DI) water. Subsequently, solvent exchange step was performed (2 × 40 mL DI water followed by 3 × 40 mL absolute methanol, with solvent refreshed every 4 h) before overnight drying under reduced pressure at ambient temperature. The reaction compositions and conditions are summarized in **Table S1**.

Table S1. Optimized reaction compositions and conditions for Zr-MOFs with Zr_{12} clusters

MOF	Metal salt (mmol)	Ligand (mmol)	Modulator (eq.)	Water (mL)	Temperature and duration
Zr_{12}-BDC-H	0.3	0.3	AA, 175	2	150 °C for 20 h
Zr_{12}-BDC-NH_2	0.6	0.6[a]	AA, 90	3	120 °C for 24 h
Zr_{12}-BDC-NO_2	0.5	0.5	AA, 120	3	150 °C for 20 h
Zr_{12}-BDC-Br	0.5	0.5	AA, 120	3	150 °C for 20 h
Zr_{12}-BDC-F_4	0.3	0.3	AA, 175	2	150 °C for 20 h

[a] Using dimethyl aminoterephthalate as the ligand yielded MOFs with better crystallinity.

Synthesis of UiO-66-NH$_2$ with Zr$_6$ clusters. Zr$_6$-BDC-NH$_2$ (i.e. UiO-66-NH$_2$) was prepared using a modified microwave procedure.[1] Briefly, $ZrOCl_2 \cdot 8H_2O$ (0.3867 g, 1.2 mmol) was dissolved in DI water (3 mL) to yield a homogeneous solution. The salt solution was then introduced into a 20 mL glass microwave reaction vial together with BDC-NH$_2$ (0.217 g, 1.2 mmol). Acetic acid (3 mL) was then added with a stirrer bar. The reaction mixture was capped and heated to 95 °C within 2 min in a microwave synthesizer (Anton Paar MW450), and held at that temperature for 1 h under stirring (800 rpm). After the reaction, the product was cooled to 55 °C under forced convection. The solids were recovered by centrifugation and subject to the same washing, drying and activation processes as described earlier.

Exfoliation and thickness measurement. To exfoliate the Zr$_{12}$ cluster-based MOFs, around 10 mg of activated MOF powder was dispersed in methanol and sonicated for 1 h. The suspension was left to sediment for 48 h before retrieving the supernatant. The supernatant solution was drop-casted on silicon wafer and dried in air at room temperature. Atomic force microscopy (AFM) measurements were performed in tapping mode in air (Bruker Dimension Icon).

Catalytic performance evaluation. Before the reactions, the MOFs underwent activation overnight at 80 °C. Varying amounts of the MOF catalysts (25 to 100 mg) were suspended into the solution of benzaldehyde dimethyl acetal (152 mg, 1.0 mmol) and malononitrile (73 mg, 1.1 mmol) dissolved in deuterated chloroform (1.5 mL). The suspension was maintained at 55 °C for 24 h under magnetic stirring in inert atmosphere. After that, the MOF catalysts were recovered by centrifugation (7000 rpm, 10 min) and the supernatant was analysed by ^{1}H NMR (Bruker, 400 MHz). For recycle experiments, the separated MOF catalysts were washed with copious amounts of water and methanol, exchanged for 4 h with absolute methanol and dried under reduced pressure at room temperature. The recovered catalysts were applied in the subsequent runs using fresh reactants and solvent.

Dissolution experiment. Quantification of the modulator to linker ratio, m_R, by dissolution NMR experiment was performed according to reference S2. Briefly, 20 mg of activated MOF sample was weighed into a 2 mL scintillation vial. The digestion medium, 1 M NaOH in D_2O, was then introduced. After sealing, the suspension was manually agitated and left standing for 24 h. The supernatant containing dissolved organic components of the MOFs was withdrawn for NMR analysis. The inorganic component is ZrO_2 and was not analysed.

Characterization. Powder X-ray diffraction (PXRD) data of all the products were collected on a Rigaku MiniFlex 600 powder X-ray diffractometer with Cu K_α radiation ($\lambda = 1.5418$ Å). The MOF samples were characterized by field-emission scanning electron microscopy (FESEM, JEOL, JSM-7610F) and transmission electron microscopy (TEM, JEOL, JEM-3010). N_2 sorption isotherms were measured on a Micromeritics ASAP 2020 at 77 K. The guest molecules in the frameworks were exchanged with fresh methanol several times before activation under vacuum (150 °C for 10 h). The thermal gravimetric analyses (TGA) were performed by using Shimadzu DTG-60AH under an air flow at a rate of 10 °C min^{-1} from 50 °C to 800 °C. Fourier transform infrared (FT-IR) spectra were obtained in attenuated total reflectance (ATR) mode on a Bruker VERTEX 70 instrument.

Synthesis optimization of Zr_{12}-BDC-NH_2

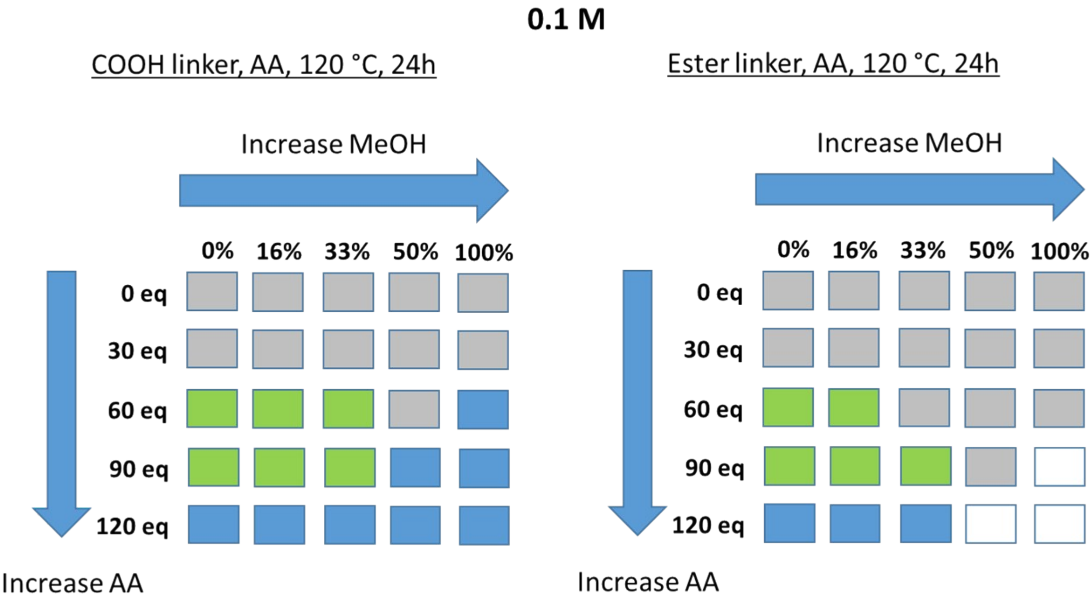

COOH linker, AA, 120 °C, 24h

	0%	16%	33%	50%	100%
0 eq	▨	▨	▨	▨	▨
30 eq	▨	▨	▨	▨	▨
60 eq	🟩	🟩	🟩	▨	🟦
90 eq	🟩	🟩	🟩	🟦	🟦
120 eq	🟦	🟦	🟦	🟦	🟦

Ester linker, AA, 120 °C, 24h

	0%	16%	33%	50%	100%
0 eq	▨	▨	▨	▨	▨
30 eq	▨	▨	▨	▨	▨
60 eq	🟩	🟩	▨	▨	▨
90 eq	🟩	🟩	🟩	▨	⬜
120 eq	🟦	🟦	🟦	⬜	⬜

Fig. S1. Dependence of cluster nuclearity in Zr-BDC-NH_2 on the solvent composition and modulator concentration: green – Zr_{12} phase; blue – Zr_6 phase; grey – amorphous gel product; white – negligible solids content.

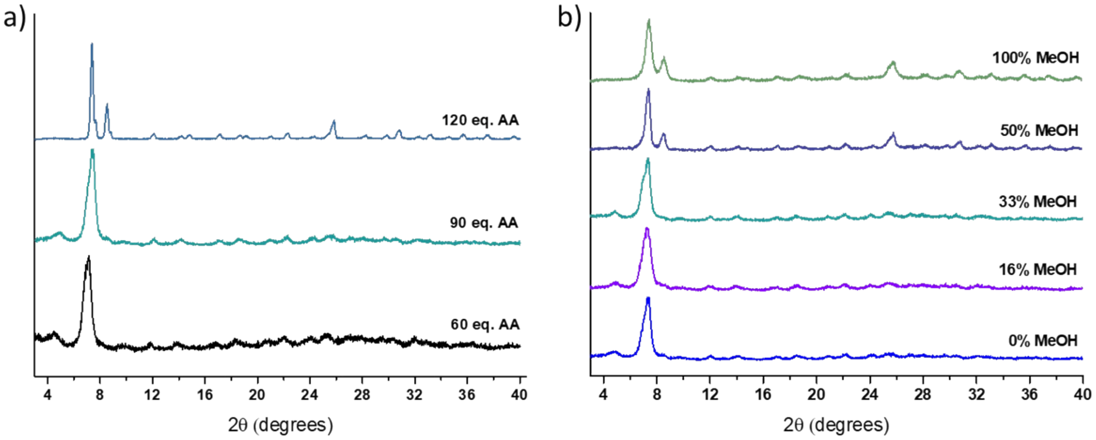

Fig. S2. PXRD patterns of Zr-BDC-NH_2 synthesized in a) varying AA concentration in 100% water solvent, b) 90 eq. AA with varying % of solvent replaced by water. The metal/linker concentration in all cases is 0.1 M, T = 120 °C, and t = 24 h.

Characterization of as-synthesized samples

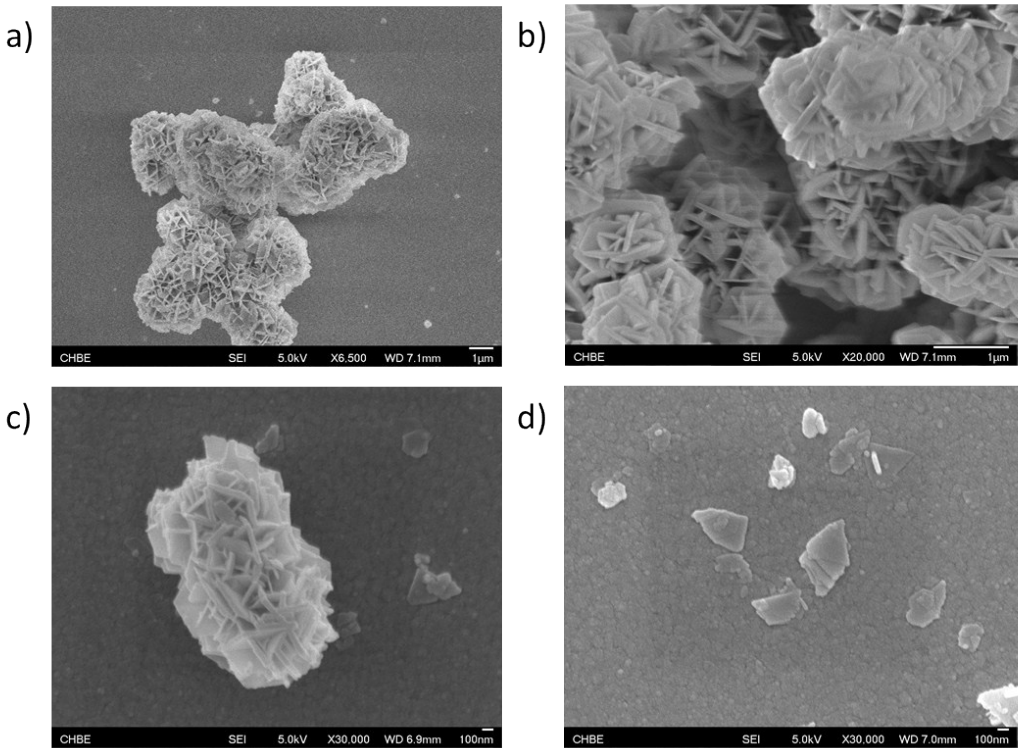

Fig. S3. SEM images of Zr_{12}-BDC-H (a, b) and Zr_{12}-BDC-NO_2 (c, d).

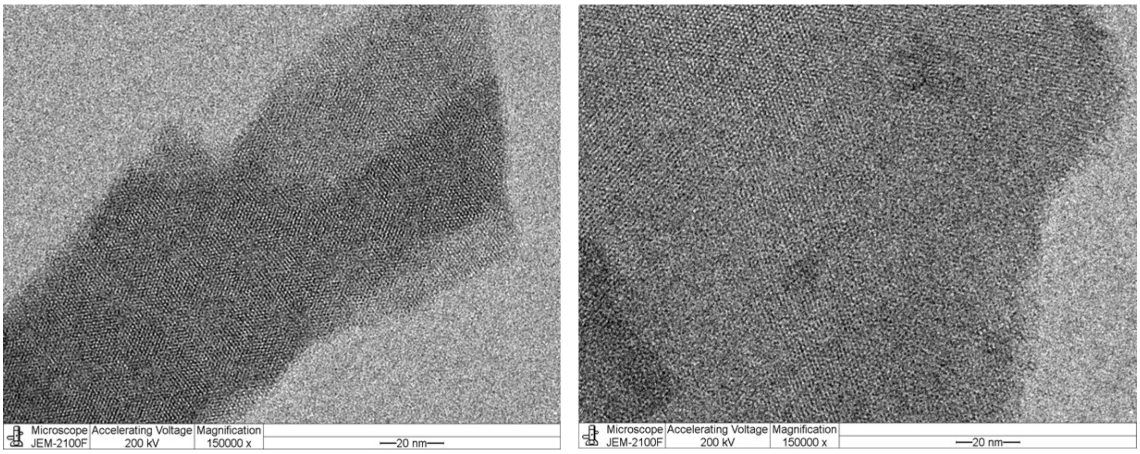

Fig. S4. TEM images of Zr_{12}-BDC-F_4 highlighting the layered structure.

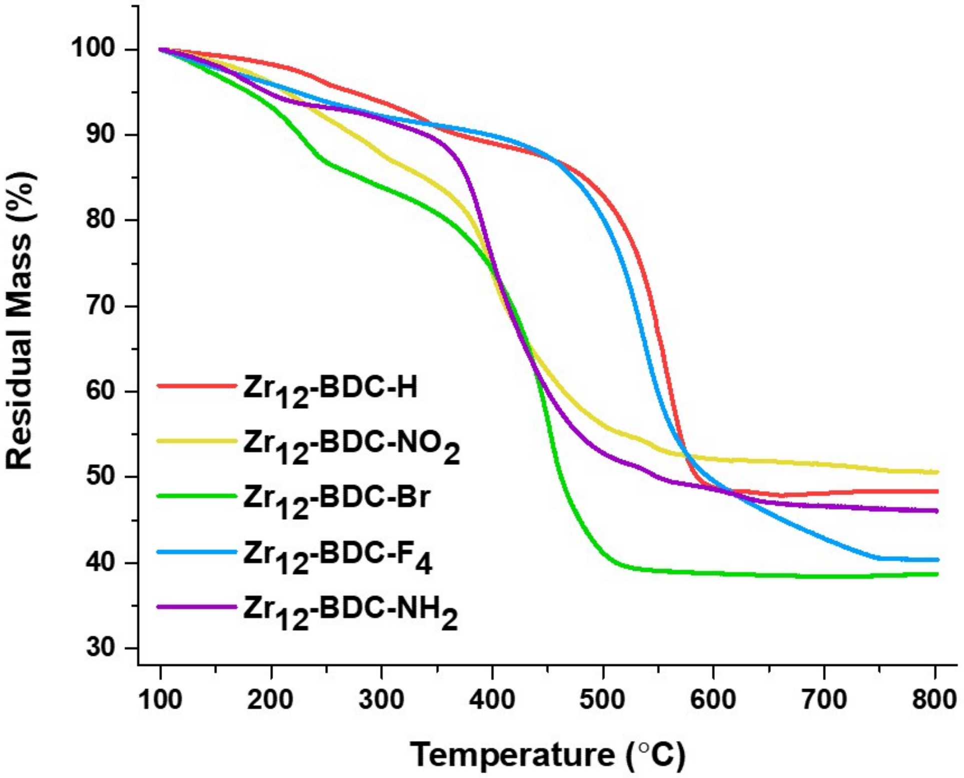

Fig. S5. TGA curves of functionalized Zr_{12}-BDC MOFs.

Table S2. BET surface areas of Zr_{12}-BDC-X determined by N_2 sorption measurements.

MOF	BET surface area (m^2 g^{-1})
Zr_{12}-BDC	622
Zr_{12}-BDC-NH_2	433
Zr_{12}-BDC-NO_2	490
Zr_{12}-BDC-Br	416
Zr_{12}-BDC-F_4	272

3D to 2D transformation of Zr_{12} cluster-based MOFs

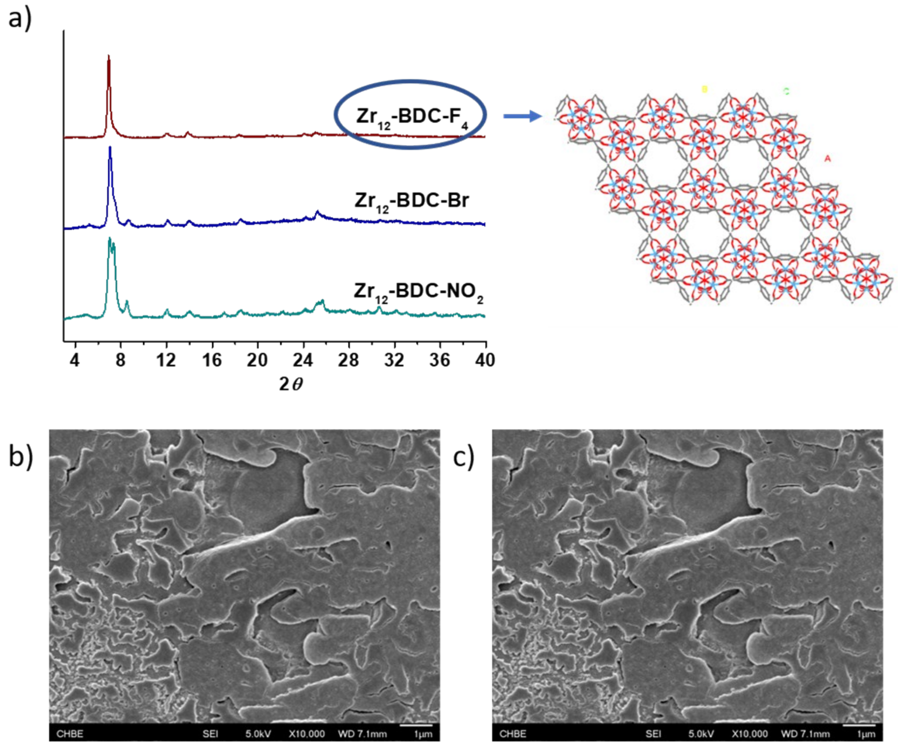

Fig. S6. (a) Spontaneous 3D-to-2D transformation of functionalized Zr_{12}-BDC. (b, c) SEM images of layered (2D) Zr_{12}-BDC-F_4.

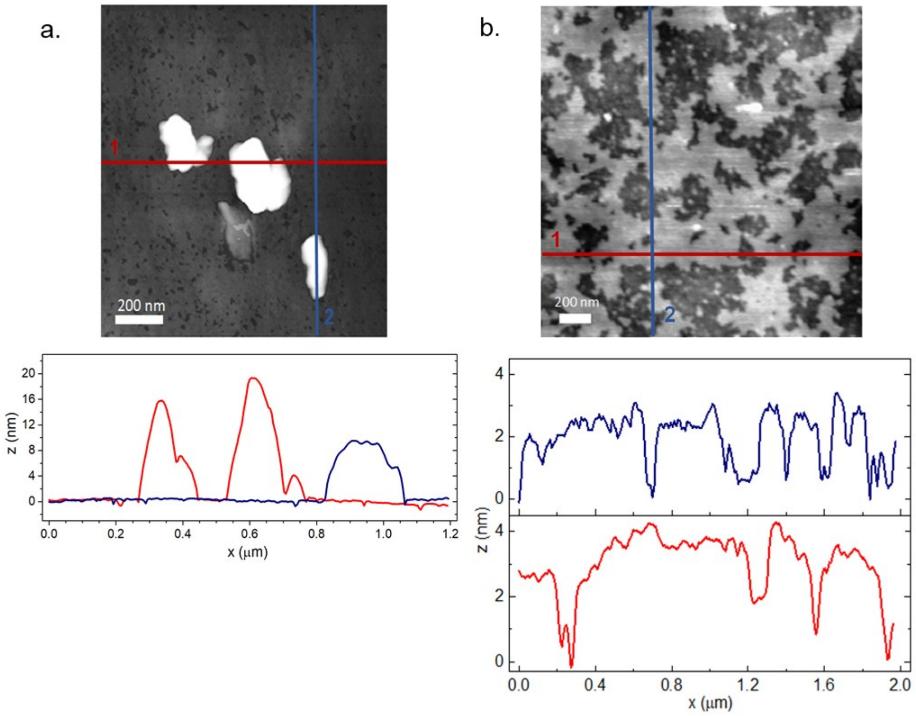

Fig. S7. AFM micrographs and line profiles of (a) Zr_{12}-BDC-NH_2 nanoparticles and (b) Zr_{12}-BDC-F_4 delaminated sheets.

Catalytic performance of Zr_{12}-BDC-NH_2

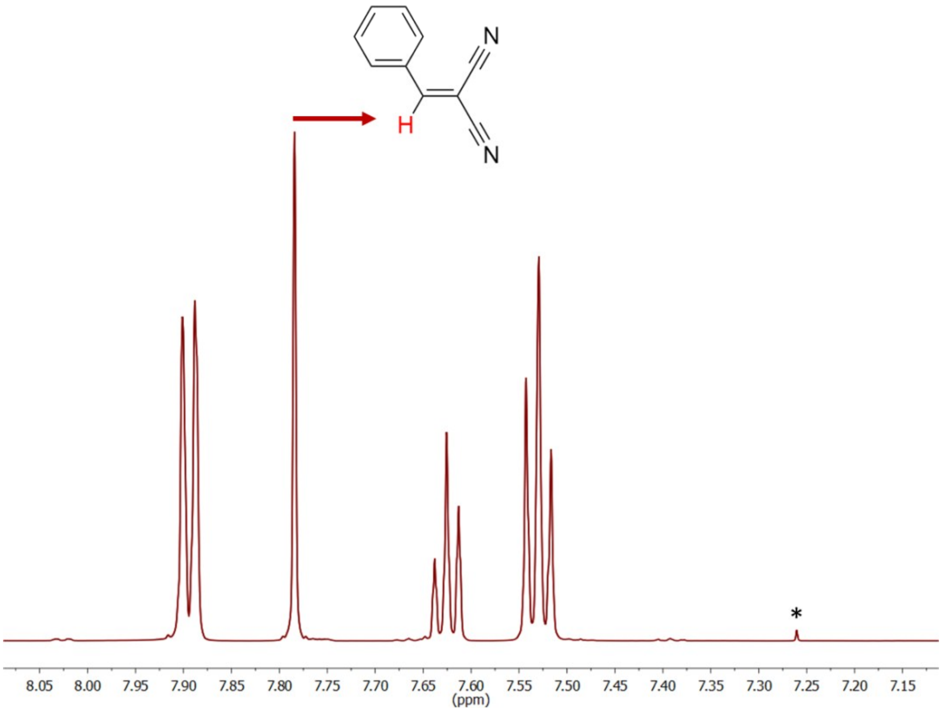

Fig. S8. ^{1}H NMR of benzylidenemalononitrile. Solvent peak ($CDCl_3$) is marked with asterisk.

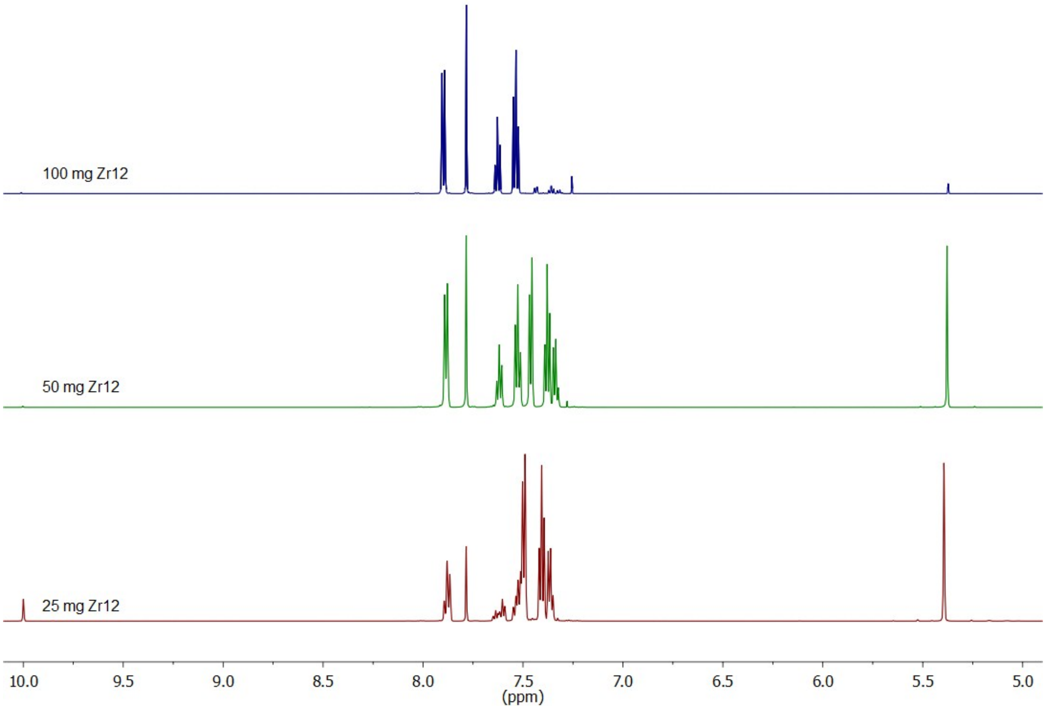

Fig. S9. Stacked ^{1}H NMR spectra of tandem deacetalization-Knoevenagel condensation catalyzed by different loadings of Zr_{12}-BDC-NH_2.

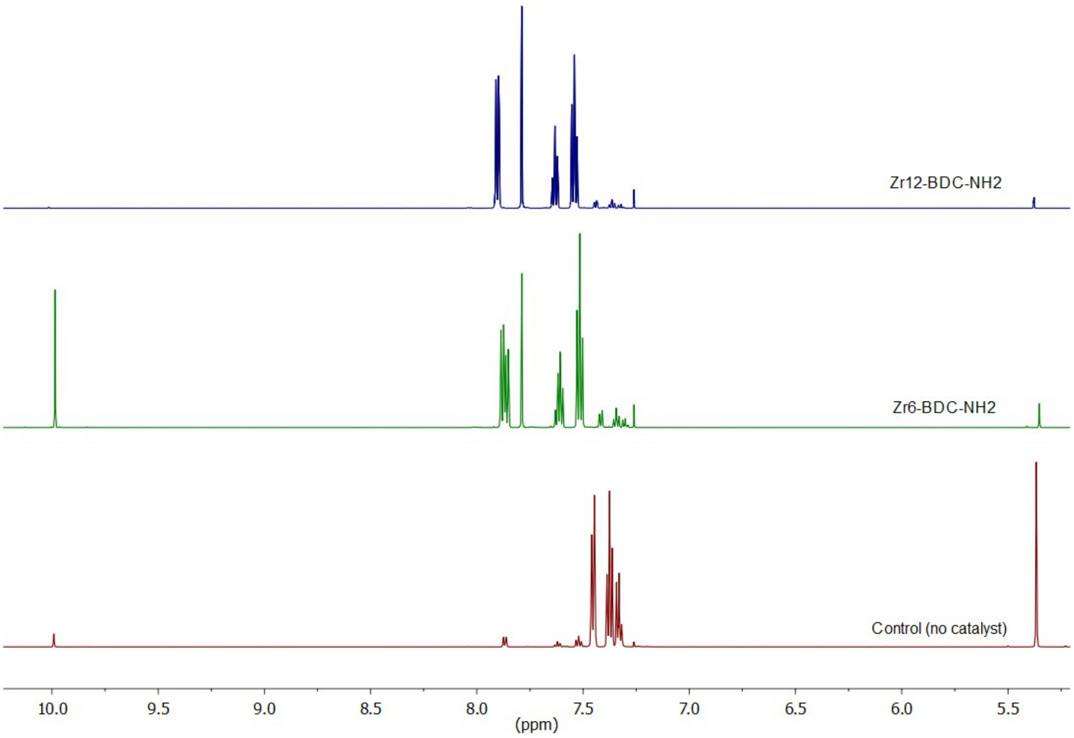

Fig. S10. Stacked ^{1}H NMR spectra of tandem deacetalization-Knoevenagel condensation catalyzed by Zr_6-BDC-NH_2 versus Zr_{12}-BDC-NH_2.

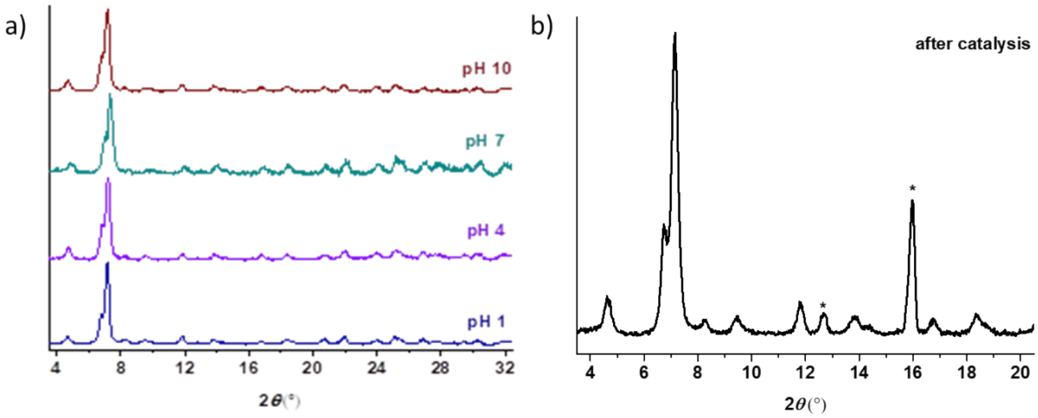

Fig. S11. Stability tests for Zr_{12}-BDC-NH_2: (a) PXRD patterns of Zr_{12}-BDC-NH_2 after soaking in aqueous solutions with various pH values for 48 h at room temperature; (b) PXRD pattern of Zr_{12}-BDC-NH_2 after a single round of catalysis. Peaks from organic impurity (benzylidene malononitrile) are marked with asterisk.

Table S3. Calculated modulator to linker ratios for Zr_{12} MOFs after digestion in 1 M NaOH/D_2O solution.

MOF	Modulator peak area	Integrated peak	Area	$\frac{Tot.mod}{BDC} m_R$
Zr_{12}-BDC-H	1.00 (3H, δ 1.84)	4H, δ 7.74	35.3	0.04
Zr_{12}-BDC-NH_2	1.00 (3H, δ 1.84)	1H, δ 7.62 dd	6.27	0.05
Zr_{12}-BDC-Br	1.00 (3H, δ 1.84)	1H, δ 7.31 dd	13.2	0.03
Zr_{12}-BDC-NO_2	1.00 (3H, δ 1.84)	1H, δ 8.43 dd	50.4	< 0.01

Table S4. Comparison of catalytic performance for tandem deacetalization-Knoevenagel condensation reaction by various catalysts.

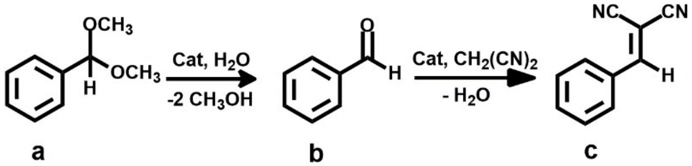

Entry	Catalyst	Loading	Solvent	Volume	Reagents	Condition	Conv. (%)	Y_B/Yc (%)	Ref.
1	Yb-BDC-NH_2	100 mg	DMSO-d_6	2 mL	2.0 mmol **a** 2.1 mmol $CH_2(CN)_2$	50 °C, 24 h	97.0	-/97.0	[3]
2	Sm-BDC-NH_2	100 mg	DMSO-d_6	2 mL	2.0 mmol **a** 2.1 mmol $CH_2(CN)_2$	50 °C, 24 h	82.0	-/82.0	
3	Dy-BDC-NH_2	100 mg	DMSO-d_6	2 mL	2.0 mmol **a** 2.1 mmol $CH_2(CN)_2$	50 °C, 24 h	76.0	-/76.0	
4	PCN-124	6 mg	DMSO-d_6	3 mL	2.0 mmol **a** 2.1 mmol $CH_2(CN)_2$	50 °C, 12 h	100	-/100	[4]
5	MIL-101-NH_2 (Al)	100 mg	1,4-dioxane	4 mL	1.0 mmol **a** 5.0 mmol $CH_2(CN)_2$	90 °C, 3 h	100	6/94	[5]
6	JUC-199	100 mg	1,4-dioxane	4 mL	1.0 mmol **a** 1.2 mmol $CH_2(CN)_2$	90 °C, 4 h	>99	-/>99	[6]
7	Fe_3O_4@HKUST-1	50 mg	1,4-dioxane	4 mL	1.0 mmol **a** 3.0 mmol $CH_2(CN)_2$	90 °C, 5 h	100	1/99	[7]

References

1. H. Reinsch, S. Waitschat, S. M. Chavan, K. P. Lillerud and N. Stock, *Eur. J. Inorg. Chem.*, 2016, **2016**, 4490-4498.
2. G. C. Shearer, S. Chavan, S. Bordiga, S. Svelle, U. Olsbye and K. P. Lillerud, *Chem. Mater.*, 2016, **28**, 3749-3761.
3. Y. Zhang, Y. Wang, L. Liu, N. Wei, M.-L. Gao, D. Zhao and Z.-B. Han, *Inorg. Chem.*, 2018, **57**, 2193-2198.
4. J. Park, J.-R. Li, Y.-P. Chen, J. Yu, A. A. Yakovenko, Z. U. Wang, L.-B. Sun, P. B. Balbuena and H.-C. Zhou, *Chem. Commun.*, 2012, **48**, 9995-9997.
5. T. Toyao, M. Fujiwaki, Y. Horiuchi and M. Matsuoka, *RSC Adv.*, 2013, **3**, 21582-21587.
6. H. He, F. Sun, B. Aguila, J. A. Perman, S. Ma and G. Zhu, *J. Mater. Chem. A*, 2016, **4**, 15240-15246.
7. T. Toyao, M. J. Styles, T. Yago, M. M. Sadiq, R. Riccò, K. Suzuki, Y. Horiuchi, M. Takahashi, M. Matsuoka and P. Falcaro, *CrystEngComm*, 2017, **19**, 4201-4210.